Geophysical Journal International

Geophys. J. Int. (2013) **193,** 187–196 doi: 10.1093/gji/ggs091

Contact impedance of grounded and capacitive electrodes

Andreas Hördt, Peter Weidelt* and Anita Przyklenk

Institute of Geophysics and Extraterrestrial Physics, TU Braunschweig, Braunschweig, Germany. E-mail: a.hoerdt@tu-braunschweig.de

Accepted 2012 November 28. Received 2012 November 22; in original form 2012 March 29

SUMMARY

The contact impedance of electrodes determines how much current can be injected into the ground for a given voltage. If the ground is very resistive, capacitive electrodes may be an alternative to galvanic coupling. The impedance of capacitive electrodes is often estimated with the assumption that the halfspace is an ideal conductor. Over resistive ground at high frequencies, however, the contact impedance will depend on the electrical properties, i.e. electrical conductivity and permittivity, of the subsurface. Here, we review existing equations for the resistance of a galvanically coupled, spherical electrode in a fullspace, and extend the theory to the general case of a sphere in a spherically layered fullspace. We then develop a method to calculate the impedance of a spherical disc over a homogeneous halfspace.

We carry out modelling studies to demonstrate the consistency of the algorithms and to assess under which conditions the determination of the electrical parameters from the impedance may be feasible. For a capacitively coupled electrode, the common assumption of an ideally conducting fullspace (or halfspace) breaks down if the displacement currents in the fullspace become as large as the conduction currents. For a moderately resistive medium with 1000 Ωm this is the case for frequencies larger than 100 kHz. The transition from a galvanically coupled disc to a disc in the air is continuous as function of distance. However, depending on the electrical parameters and frequency, the impedance may vary by several orders of magnitude within a few nanometers distance or less. We derive a simple equation to assess under which conditions the impedance is independent of the electrode height, which may be important for determining subsurface permittivity and conductivity in cases where control on the exact geometry is difficult. Our theory is consistent with measured data obtained in a sandbox in the laboratory.

Key words: Numerical solutions; Electrical properties; Electromagnetic theory; Glaciology; Hydrogeophysics.

1 INTRODUCTION

DC resistivity measurements are usually carried out with four electrodes. This way, the ratio between measured voltage and injected current is independent of the grounding resistance of the electrodes. However, the estimation of the electrode resistance may be important in some situations. If the ground is very resistive, technical issues such as maximum transmitter voltage and signal stability may limit the current that can be injected into the ground. When trying to decrease contact resistance, for example by watering electrodes, the dependence on ground resistivity or geometry is important to find an efficient strategy.

The capacitive resistivity technique uses capacitive electrodes, which normally consist of sheets close to the ground with no direct contact. They are used with an alternating current of high frequency such that the impedance is sufficiently low. The method may be particularly useful if the ground is very resistive and galvanic coupling is not feasible, or if fast measurements with a moving system are to be carried out (Kuras *et al.* 2007). The capacitive resistivity technique is also attractive to determine electrical parameters of small bodies in the solar system from landers (Grard & Tabbagh 1991; Seidensticker *et al.* 2007; Spitzer *et al.* 2008).

To estimate the contact impedance of capacitive electrodes, the halfspace is often assumed to be an ideal conductor. For example, Kuras *et al.* (2006) considered electrical conductivity and permittivity when calculating the transfer impedance of their four-electrode configuration, but used the ideal-conductor approximation to estimate contact impedances. Over very resistive ground, however, the assumption of an ideal conductor is no longer valid, and the impedance of capacitive electrodes will also depend on electrical conductivity and dielectric permittivity of the halfspace. This dependence might in principle be used to determine the electrical parameters directly from the contact impedance. In that case, the sensitive depth range is controlled by the electrode size rather than by their distance. Such measurements might be useful for very

* Deceased.

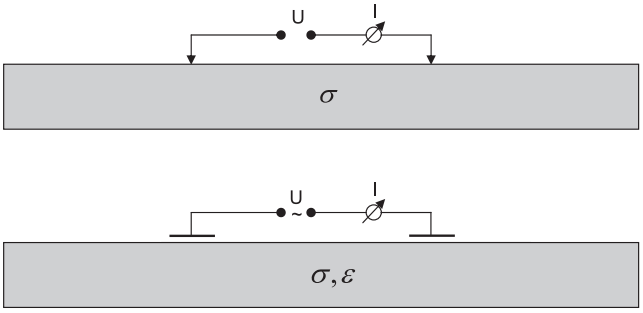

Figure 1. Sketch of the basic setup. Top panel: DC voltage applied to galvanically coupled electrodes. Bottom: AC voltage applied to capacitively coupled electrodes.

shallow penetration, or to supplement information that is obtained from the standard 4-point transfer impedance. Dashevsky *et al.* (2005) describe a system where the vertical derivative of the impedance is used to evaluate asphalt pavement quality from electrical permittivity. They solve the underlying equations numerically and study the sensitivity of the measured impedance with respect to parameters of a layered model.

The impedance of electrodes is treated to some extent in textbooks (e.g. Krajew 1957; Smythe 1968), and different solutions were derived using approximations and electrode geometries with particular applications or frequency ranges in mind (e.g. Wait & Pope 1954; Maley & King 1961). Here, we study the impedance of spherical and disc electrodes over a halfspace with respect to geophysical applications, and discuss some properties relevant for the design of measurement systems and the determination of subsurface parameters. We review existing equations for galvanically coupled spherical electrodes in a fullspace and extend the theory to capacitively coupled spheres. We derive a new semi-analytical solution for the impedance of a circular disc electrode over a halfspace. We investigate under which conditions the measurement of contact impedance might be feasible to determine conductivity and dielectric permittivity of the ground, and thus might constitute an alternative or useful supplement to conventional transfer impedance measurements.

2 THEORY

The setup describing the problem to be solved is sketched in Fig. 1. A DC or AC voltage is applied to galvanically coupled electrodes (top panel) or an AC voltage to capacitively coupled electrodes (bottom panel). The aim is to derive equations for the contact impedance Z, required to calculate the current I from the applied voltage U via:

$$Z = U/I, \tag{1}$$

where Z depends on resistivity for galvanic coupling, and on resistivity and electric permittivity in the case of capacitive coupling.

2.1 Spherical electrode in a fullspace

The calculation of the impedance of arbitrary electrodes over a halfspace depends on the shape of the electrodes and requires a numerical solution (e.g. Rücker & Günther 2011). As a first step, we consider the simple problem of a spherical electrode in a fullspace. For this case, analytical solutions exist which are useful to obtain physical insight and can be used to verify the numerical solution derived later for circular disc electrodes. We assume a single electrode with a given potential V_0 with respect to infinity, surrounded by two

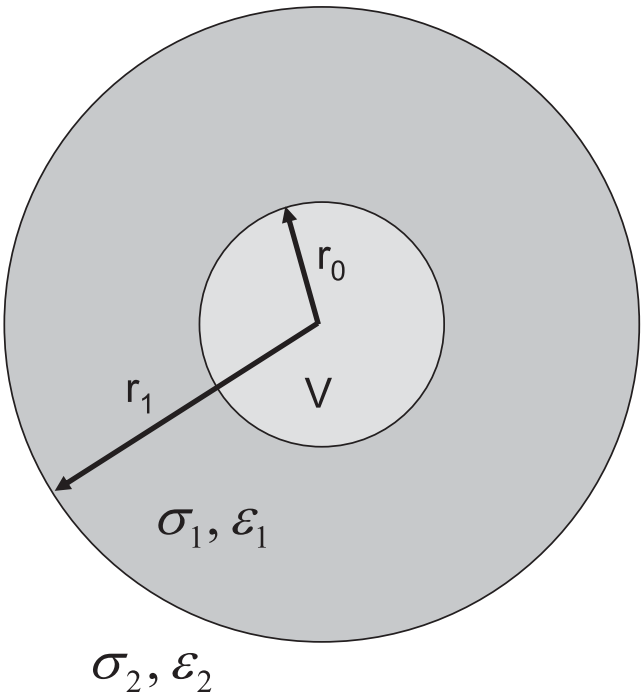

Figure 2. Sketch defining the parameters of a spherical electrode in a two-layered halfspace.

shells, where the outer shell is infinitely thick. Both shells are characterized by an electrical conductivity σ and dielectric permittivity ϵ. The geometrical parameters are defined in Fig. 2. Krajew (1957) calculated the impedance for the case of a DC current and galvanic coupling. In that case, the impedance is real and is called resistance, independent of the permittivities of the two shells:

$$R = \frac{1}{4\pi}\left(\frac{1}{\sigma_2 r_1} - \frac{1}{\sigma_1 r_1} + \frac{1}{\sigma_1 r_0}\right). \tag{2}$$

The resistance of a two-electrode system, where the voltage equals the potential difference between the two electrodes, can be obtained by simply adding the resistances of the single electrodes, provided that the distance between the electrodes is large compared to their size. If they are close to each other, mutual influence of the charges will affect the charge distribution on the electrodes, and thus the impedances. The mutual influence provides an additional term that decays with $1/L$, where L is the electrode distance (Krajew 1957; Smythe 1968). We will also use this approximation later during the derivation of the impedance of a circular disc. Note that there is nothing like a 'resistance of the ground between the two electrodes', and the total impedance does not depend on the distance between the electrodes as soon as the distance is large compared to their size.

Eq. (2) can be extended to the AC case by introducing the complex conductivity

$$\bar{\sigma} = \sigma + i\omega\varepsilon, \tag{3}$$

where ω is the angular frequency. For a spherical electrode, it can be shown from Maxwell's equations that the equation for the potential V of the electric field is

$$\nabla \cdot (\bar{\sigma} \nabla V) = 0. \tag{4}$$

This is the same equation that is used to derive eq. (2) except that the real conductivity was replaced by its complex form. Therefore,

the subsequent derivation also holds in the complex case, and the resistance becomes a complex impedance written as:

$$Z = \frac{1}{4\pi}\left(\frac{1}{\bar{\sigma}_2 r_1} - \frac{1}{\bar{\sigma}_1 r_1} + \frac{1}{\bar{\sigma}_1 r_0}\right). \tag{5}$$

This equation may be used to calculate the impedance of a galvanically coupled electrode, where $\sigma_1 \neq 0$, or a capacitively coupled electrode, where the medium surrounding the electrode would be air. In the latter case, $\sigma_1 = 0$, and $\varepsilon_1 = \varepsilon_0$, where ε_0 is the free-space permittivity. If the fullspace surrounding the electrode (the second medium) is sufficiently conductive, the common ideal conductor assumption will hold, and the resistance will not depend on the electrical parameters of the fullspace. This can be seen by writing eq. (5) in the limit $\sigma_2 \to \infty$:

$$Z = \frac{r_1 - r_o}{i\omega\varepsilon_o 4\pi r_0 r_1}, \tag{6}$$

which is identical to the known equation for a spherical capacitor (Smythe 1968).

2.2 Circular disc over a homogeneous halfspace

For a disc electrode over a homogeneous halfspace, the impedance is equal to that of a plate capacitor, if the halfspace is conductive, and the distance d between halfspace and disc is small compared to the size of the disc (Smythe 1968):

$$Z = \frac{d}{i\omega\varepsilon_o A} = \frac{1}{i\omega C}, \tag{7}$$

where A is the area of the disc, and C is the capacitance. For arbitrary distances and halfspace conductivities, no analytical solution in compact form exists. We derive an integral equation and solve it numerically for the case of an infinitely thin disc in the air or directly on a conductive halfspace. The geometrical parameters are defined in Fig. 3. The ideally conducting disc with radius a is parallel to the surface at a height d above the surface. The coordinate system is chosen with the origin at the centre of the disc. Harmonic time dependence is assumed.

The strategy to find the impedance is to calculate the charge on the disc for a given potential V_0. The charge distribution will be radially symmetric and may be described by a charge per unit length density that depends only on the radial distance $q(r)$. The total charge Q is then obtained from

$$Q = 2\pi \int_0^a q(s)\, ds. \tag{8}$$

Having obtained Q, the complex capacitance can be calculated from

$$C = \frac{Q}{U} \tag{9}$$

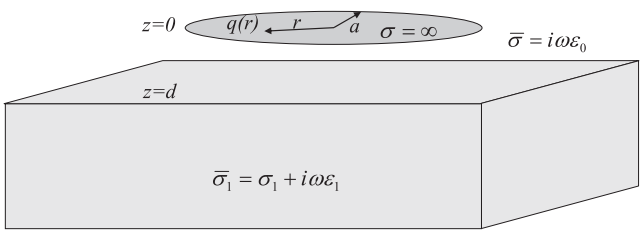

Figure 3. Sketch defining the parameters of a circular disc over a homogeneous halfspace. The radius is denoted by a, d is the electrode height, and $q(r)$ is the charge per unit length density on the disc.

and the complex impedance is obtained from eq. (7). The condition of an infinite conductivity, and thus a constant potential on the disc, means that the electric field is zero. The solution strategy is to express the radial electric field E_r as function of $q(r)$ using Maxwell's equations and determine $q(r)$ such that E_r vanishes anywhere on the disc. The full derivation is given in the appendix, where we obtain the following equations to determine $q(r)$:

$$\frac{1}{2\varepsilon_0}\int_0^a sq(s)\, F(s,r)\, ds = 0, \tag{10}$$

where

$$F(s,r) = \int_0^\infty u\left[1 - R(u)\, e^{-2ud}\right] J_0(us)\, J_1(ur)\, du. \tag{11}$$

Here, the integration variable u is the spatial wavenumber and J_1 and J_0 are Bessel functions, $R(u)$ is a reflection factor which depends on the electrical parameters of the halfspace, and is given in the appendix.

Eq. (10) has to be solved under the condition that

$$\frac{1}{\varepsilon_0}\int_0^a sq(s)\, G(s) ds = V_0, \tag{12}$$

where

$$G(s) = \int_0^\infty \left(1 - R(u)\, e^{-2ud}\right) J_0(us)\left[J_0(ua) - J_0(u(L-a))\right] du. \tag{13}$$

The charge density is calculated as the solution of the linear equation system that is obtained from eqs (10) and (12) by discretizing the disc along the radial direction. L is the distance between two electrodes with $L > 2a$ that may be chosen freely for the numerical implementation. The only approximation that is made during the derivation is that the radius of the disc is small compared to the electromagnetic wavelength in free space, which does not constitute a limitation in practical situations.

3 RESULTS

3.1 Galvanically coupled spherical electrode

The contact impedance of a galvanically coupled electrode based on eq. (2) or others in similar form has been studied by several authors, including different electrode shapes (e.g. Krajew 1957; Rücker & Günther 2011). Here, we investigate the sensitivity of the impedance with respect to the conductivity in the volume surrounding the electrode. It is common practice to decrease contact resistance by pouring water into the ground near the electrode, and we may estimate the amounts of water and the conductivity contrast which is required to achieve a certain reduction in resistance. We assume that the water fills a spherical shell of radius r_1 and increases the conductivity to σ_1 compared to σ_2 of the undisturbed formation. The decrease of contact resistance may be expressed by normalization with the fullspace value:

$$\frac{R}{R_0} = \frac{r_0}{r_1} - \frac{\sigma_2 r_0}{\sigma_1 r_1} + \frac{\sigma_2}{\sigma_1}, \tag{14}$$

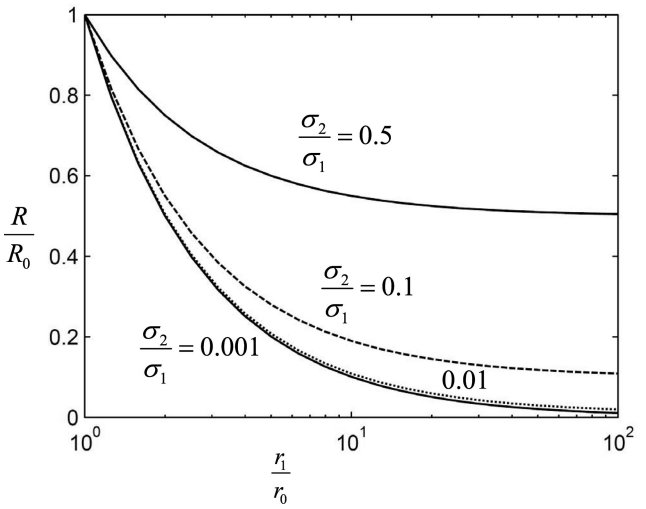

Figure 4. Normalized electrode resistance as function of normalized radius of the conductive shell for different conductivity ratios between outer fullspace and conductive shell. Note the logarithmic radius axis.

where

$$R_0 = \frac{1}{4\pi\sigma_2 r_0} \tag{15}$$

denotes the resistance in a fullspace with conductivity σ_2. The fullspace resistance is obtained from eq. (2) by setting $r_1 = r_0$, and may be considered the case where no electrode watering was applied.

Fig. 4 illustrates the reduction of electrode resistance by a conductive spherical shell surrounding the electrode. The resistance quickly decreases with the size of the conductive shell, but for radii larger than 10 times the electrode size, a further increase is not efficient any more. For example, for a conductivity contrast of 0.1, an increase of the radius ratio from 10 to 100, corresponding to a volume increase by a factor of 1000, will only decrease resistance by a factor of 2. The impedance also saturates with respect to conductivity contrast. Once a contrast of approx. 0.1 is reached, a further decrease does not lead to a significant decrease of resistance. For example, there is no need to use a highly saline solution of 100 S m^{-1} to decrease contact impedance if the medium is saturated with 0.01 S m^{-1} fresh water; a 1 S m^{-1} solution would have the same effect.

Eq. (14) is also useful to assess the contact resistance measurement as a method to determine the resistivity of the subsurface. Fig. 4 shows that mainly the range up to 10 times the electrode radius determines the contact impedance, i.e. if the thickness of the inner shell is larger than 10 electrode radii, a further increase changes contact impedance only marginally. Thus, 10 electrode radii may be considered an approximate sensitivity range.

3.2 Capacitively coupled circular disc

When designing a capacitive electrode, it is important to estimate its impedance, because it will determine the magnitude of the required voltage and the current that can be achieved. If the ground is sufficiently conductive, the approximation of an ideal conductor (eq. 7) may be used. Over resistive ground, the approximation will not be valid any more. The transition is illustrated in Fig. 5, which was generated by applying the numerical implementation of the scheme described in the theoretical section to calculate the impedance of the circular disc. The figure shows the magnitude

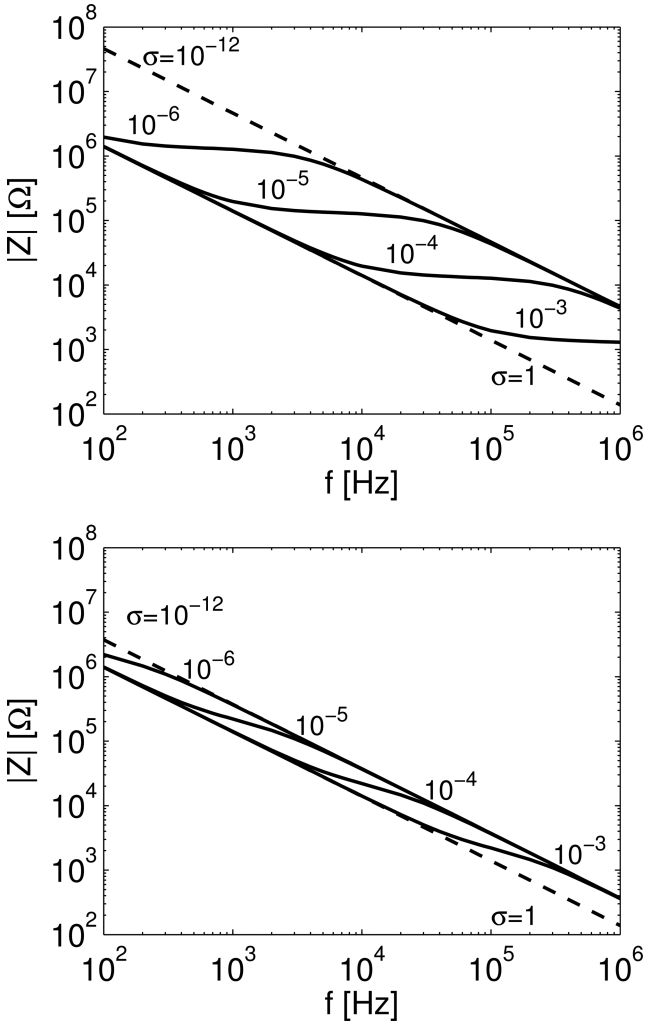

Figure 5. Magnitude of the impedance of a capacitively coupled circular disc electrode over a homogeneous halfspace vs. frequency, for different conductivities (in S m^{-1}) of the halfspace. Top panel: with a relative permittivity of the halfspace fixed to $\varepsilon_r = 4$. bottom panel: $\varepsilon_r = 100$. The radius of the disc is 0.2 m, the distance between disc and halfspace is 1 mm. The upper and lower dashed curves denote the limits of infinite and zero halfspace conductivities, which cannot be distinguished from the corresponding finite values.

of the impedance vs. frequency for varying electrical conductivity of the halfspace, for two different permittivities (4 and 100). The upper dashed curve with extremely small conductivity corresponds to the non-conducting case, where the coupling takes place purely through displacement currents. If a relative permittivity of 1 had been chosen (instead of 4 or 100), this would correspond to the plate in the air.

The lower dashed curve denotes the case of an ideal conductor with the $1/\omega$ frequency dependence as described by eq. (7). In the figure, it cannot be distinguished from the 1 S m^{-1} curve. If the halfspace is moderately resistive (i.e. $\sigma = 10^{-3}$ S m^{-1}), the impedance starts to deviate from the ideal conductor limit at approx. 100 kHz. For very small conductivities (i.e. $\sigma_2 = 10^{-6}$ S m^{-1}), the transition starts at relatively low frequencies around 100 Hz. Of course, the transition frequency corresponds to the point where displacement currents start to become as large as conduction currents. Therefore, in the lower panel, where a larger halfspace permittivity was chosen, the transition starts at lower frequencies. Obviously, if a capacitive

electrode system is used over permafrost areas, over very dry rock, or on space missions landing on asteroids or comets, the ideal conductor equations will break down, and the full equations have to be used to estimate electrode impedance.

For simplicity, the relative permittivity of the ground was chosen to be independent of frequency in Fig. 5. In reality, it varies with frequency, and also depends on the composition and state (frozen or unfrozen) of the material. In general, it decreases with frequency within the range investigated here (e.g. Chelidze *et al.* 1999; Lesmes & Morgan 2001; Stillman *et al.* 2010). The two values in the figure were chosen to illustrate the effect of changing permittivity, with $\varepsilon_r = 4$ representing a lower extreme, and $\varepsilon_r = 100$ being a more realistic value. When permittivity is increased, the influence of conductivity on the impedance magnitude is diminished. The curves move closer towards the ideally conducting case, because the perfect coupling, where the contact impedance depends only on geometry, can also be achieved through displacement currents. This can also be seen from an approximate equation discussed further below.

The distance to the ground is another important parameter of a capacitively coupled electrode. With the ideal conductor approximation, the impedance magnitude increases linearly with distance. However, this approximation will break down for small conductivities and large distances, and the full equations have to be considered. Also, in the limit of zero distance, corresponding to an electrode on the ground, the approximation predicts zero impedance, whereas in reality it will have a finite value. Therefore, we display the impedance magnitude vs. electrode distance for different ground conductivities in Fig. 6. The frequency is 10 kHz, and two different values of the relative permittivity (4 and 100) were chosen. The impedances of the spherical electrode were calculated using the analytical solution (eq. 5), those of the circular disc were calculated by applying the numerical implementation.

We use both the analytical equation for a spherical electrode in a fullspace and for a circular disc over a halfspace, in order to verify the numerical implementation. The results cannot agree exactly over the entire distance range, because the sphere and the disc are fundamentally different systems. However, they agree in a range of distances that depends on the normalization of the electrode surface. Here, we chose the radii such that the surface of the spherical electrode is equal to a single side of the disc. In this case, the results should be identical in the intermediate distance range, if coupling to the ground dominates over coupling to the air. The ideal conductor approximation holds and the geometries may be compared through eqs (6) and (7). Fig. 6 shows that the impedances of the disc and sphere agree indeed in the intermediate range, which we consider evidence for a successful numerical implementation.

At large distances, the disc and sphere electrodes converge to their respective vacuum value. For a sphere with radius r_0 this is (Smythe 1968):

$$Z = \frac{1}{4\pi i \omega \varepsilon_o r_0} \tag{16}$$

and for a disc with radius a:

$$Z = \frac{1}{8 i \omega \varepsilon_o a} \tag{17}$$

If $a = 2r_0$, as we adopted for the calculation in Fig. 6, the vacuum impedance of the disc is smaller than that of a sphere, because with this normalization the two-sided surface of the disc is larger.

In the limit of small distances, the comparison depends on the conductivity and permittivity of the medium. For moderate conductivities ($\sigma = 10^{-4}$ and 10^{-1} S m^{-1}), the impedance magnitude converges towards the value of a disc with zero distance, i.e. direct contact, given by

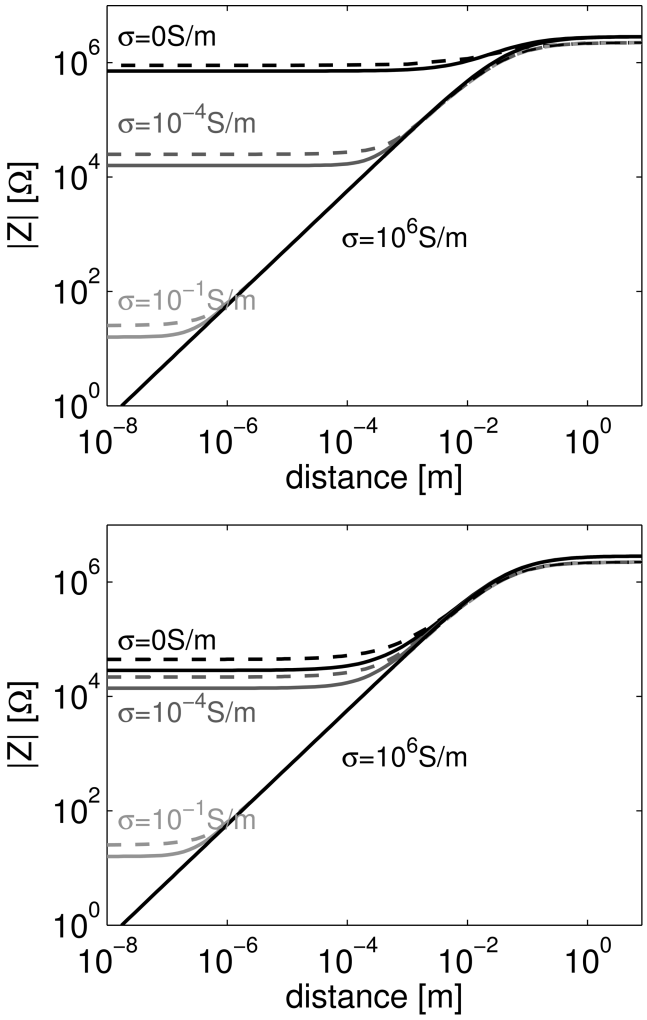

Figure 6. Impedance magnitude of the capacitively coupled spherical and circular disc electrode vs. distance to the surrounding sphere/halfspace, respectively. The solid lines indicate the impedance of the spherical electrode in fullspace, with radius 0.05 m. The dashed lines are the impedance of the circular disc electrode with radius 0.1 m. The frequency is 10 kHz, the relative permittivity of the subsurface is $\varepsilon_r = 4$ (top panel) and $\varepsilon_r = 100$ (bottom panel).

$$Z = \frac{1}{4\pi \bar{\sigma} r_0} \tag{18}$$

for the sphere and

$$Z = \frac{1}{4a} \frac{1}{\sigma + i\omega(\varepsilon_0 + \varepsilon_1)} \tag{19}$$

for the disc.

In this case, the impedance of the disc is a little larger than that of the sphere if the contact surfaces are the same ($a = 2r_0$). For very large conductivities in the range of metal ($\sigma = 10^6$ S m^{-1}), the limit is not reached even at extremely small finite distances. For zero conductivity the coupling takes place through displacement currents only. The impedance decreases with distance, because $\varepsilon_r > 1$ was chosen and the halfspace/fullspace contributes to the coupling. The dependence on permittivity, i.e. the difference between the two

panels in Fig. 6, is only visible for small to moderate conductivities ($\sigma = 0$ and 10^{-4} S m^{-1}). With increasing permittivity, the lower limit of the impedance magnitude decreases.

In summary, all curves show the expected behaviour. In the intermediate distance range, only the areas of the electrodes facing the halfspace/fullspace are relevant. In the limit of very large and very small distances, the analytical values of vacuum and galvanically coupled electrode are reached, which are different for a sphere and a disc.

Two important conclusions are illustrated in Fig. 6. First, the impedance increases monotonically with distance. This includes the case of a galvanically coupled electrode touching ground. Therefore, an electrode in the air can not have a smaller impedance than that of the same electrode lying on the ground. Second, the transition from a galvanically coupled electrode towards a capacitively coupled electrode is continuous. This might be counterintuitive; one could expect a jump in impedance when the electrode is lifted from the ground. The behaviour can be understood by considering the total impedance as the sum of two components: the ground impedance of a touching electrode, and the impedance of the space between electrode and ground that must be overcome by capacitive coupling. The latter continuously vanishes for small distance. However, Fig. 6 also shows that, depending on the electrical parameters of the ground, the transition may take place at extremely small spatial scales less than an atomic radius, and thus will appear as a discontinuity in experiments, depending on their spatial resolution.

For a spherical electrode, the interpretation of the impedance as a series connection between the ground impedance and the capacitive coupling becomes directly obvious from eq. (5), which may also be written as:

$$Z = \frac{1}{4\pi\bar{\sigma}_2 r_1} + \frac{r_1 - r_o}{i\omega\varepsilon_o 4\pi r_0 r_1} \tag{20}$$

This suggests that at small distances, the impedance of the circular plate may be written in a similar form:

$$Z = \frac{1}{4a\,(\sigma + i\omega\,(\varepsilon_0 + \varepsilon_1))} + \frac{d}{i\omega\varepsilon_0\pi a^2} \tag{21}$$

where the first term represents the grounding impedance and the second the ideal conductor capacitive coupling impedance. Indeed, eq. (21) is a good approximation in the range $d \ll a$ in Fig. 6.

Eq. (21) is also useful to understand the difference between the two panels in Fig. 5 discussed earlier. When permittivity (ε_1) is increased, the first term in eq. (21) decreases and the curves converge towards the second term, the ideally conducting limit.

The interpretation of the electrode impedance as a sum of a 'grounding impedance' and the capacitive coupling does not contradict the statement made earlier that no additional impedance of the space 'between the electrodes' exists. Eqs (20) and (21) are valid for single electrodes, and the impedance of a two-electrode system can be obtained by superposition, which constitutes a complete description.

When attempting to determine the electrical parameters of the ground from the contact impedance, for example to supplement conventional measurements with a four-electrode configuration, we have to distinguish two situations. If the electrode has a direct contact ($d = 0$), conductivity and permittivity may directly be calculated from the real and imaginary parts. Depending on the magnitude of displacement and conduction currents, it may be possible to determine only one of the parameters. For example, if conduction currents are large ($\sigma \gg \omega\varepsilon$), the magnitude of the impedance will depend on conductivity only, and the phase shift might be too small to be measured.

The ideal case of $d = 0$ will rarely be fulfilled, because either a capacitive electrode at finite distance from the ground is used, or not all parts of an electrode will be touching ground. In that case, the electrical parameters can still be determined from the contact impedance if the distance is so small that the impedance does not depend on it, i.e. the measurements are carried out in the asymptotic range at the left side of Fig. 6. This range will also determine the maximum thickness that should be used for the insulation of a capacitive electrode, or the maximum spatial scale of roughness of the electrode contact. A condition can be derived from eq. (21) by requesting that the magnitude of the second term is small compared to the first, resulting in:

$$d << a\frac{\pi}{4}\sqrt{\frac{1}{\left(\frac{\sigma}{\omega\varepsilon}\right)^2 + (1+\varepsilon_r)^2}}, \tag{22}$$

where ε_r is the relative permittivity of the halfspace. For example, for the parameters chosen for Fig. 6 (top panel), and $\sigma = 0.1$ S m^{-1}, eq. (22) yields $d \ll 4{\cdot}10^{-7}$ m, corresponding to the transition zone for the 0.1 S/m curve. For $\sigma = 0$, eq. (22) yields, $d \ll 0.015$ m, which defines the transition zone of the 0 S m^{-1} curve. In general, over resistive ground the impedance is less sensitive to electrode distance than over conductive ground.

3.3 Comparison with measured data

We carried out preliminary contact impedance measurements with a prototype impedance spectrometer built by Lippmann Geophysikalische Messgeräte (LGM), particularly designed to measure large impedances at four frequencies between 100 Hz and 100 kHz. The measurements were carried out in a box filled with dry sandy gravel with dimensions 1.2 m × 1.2 m × 0.8 m. The resistivity of the material was determined to be approx. 25 kΩm with a conventional four-electrode system; the permittivity is unknown. The two electrodes consist of circular plates of 6.5 cm radius, and a 50-μm thick insulation. Fig. 7 shows the measured single-electrode

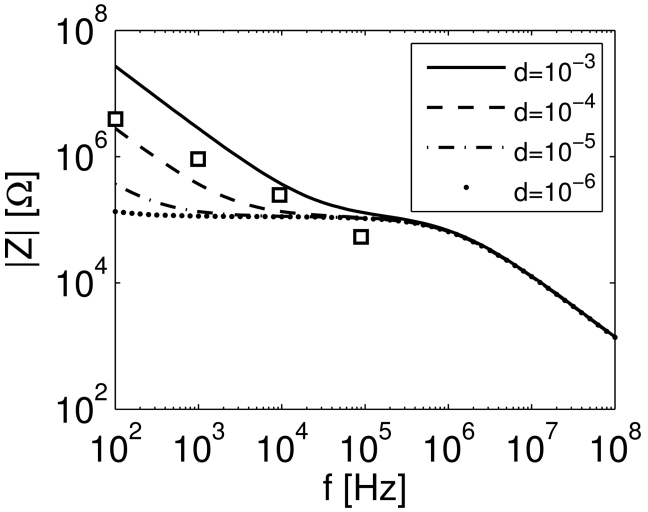

Figure 7. Measured impedance magnitudes (squares), for a system consisting of two circular electrodes with 50-μm insulation pressed on dry sandy gravel. The lines are theoretical curves calculated for varying distance to the ground (given in m). The assumed ground resistivity is 25 kΩm, and the frequency-dependent permittivity is defined by $\varepsilon_r = 10^6$ f^{-1}, where f is given in Hz.

impedance magnitudes, obtained as half of the total impedance, compared with theoretical curves calculated for different assumed distances between the ground and the electrodes.

The comparison between measured and calculated data is not trivial, because important parameters are not known or not easy to determine. The insulated electrodes were touching the sand, but it turned out that the impedance depends on the pressure at which the electrode is pushed down. This is probably because the geometry of the sand grains is changed when pressing, and distance changes in the hundreds of micrometer range are relevant. To compare with calculated data, where a planar surface is assumed, one would have to work with an effective distance, which is probably slightly larger than the thickness of the insulation (5×10^{-5} m). Also, the permittivity of the material is unknown and frequency-dependent and may vary by several orders of magnitude in the considered frequency range. We chose a function of $\varepsilon_r = 10^6\ \mathrm{f}^{-1}$, where f is given in Hz, as a rough estimate according to the corresponding literature (e.g. Lesmes & Morgan 2001). Considering those uncertainties, theoretical and measured data compare quite well.

The dependence of the impedance on distance for the theoretical data, and on pressure for the measured data, means that it would actually be difficult for this parameter set to estimate electrical parameters by inversion. The fact that the influence of distance increases at low frequencies is solely due to the assumed frequency-dependence of permittivity, which can be seen from eq. (22). For the chosen parameters, the first term under the square root can be neglected against the second one, and the threshold below which distance becomes unimportant is:

$$d \ll \frac{a}{\varepsilon_r(f)}\frac{\pi}{4}. \tag{23}$$

This yields 5μm at 100 Hz. At this frequency the selected distances in the figure do not fulfill the condition (23), and the impedance depends on distance. At 100 kHz, the equation yields 5 mm, and the condition (23) is fulfilled except for the larges selected distance (1 mm). Therefore, the largest frequency would be best suited to estimate electrical parameters. The example illustrates that careful choice of measurement parameters is recommended when attempting to estimate electrical properties from contact impedance.

4 CONCLUSIONS

We investigate the behaviour of the contact impedance of electrodes using analytical equations for spherical electrodes in a fullspace, and for a thin circular disc over a homogeneous halfspace. For the disc model, we have developed a numerical algorithm based on the full solution of Maxwell's equations. We use the approximation that the radius of the disc is small compared to the electromagnetic wavelength in free space. This will break down only for extremely high frequencies and large discs, and does not constitute a limitation in most practical situations. The code was verified by comparison with an analytical solution for a spherical electrode, and with asymptotic solutions reached in the limit of small and large distances to the halfspace. We also compared the results with measured data and obtained a reasonable agreement considering uncertainties in the parameters of the experiment.

For a galvanically coupled, spherical electrode at DC we studied the sensitivity of electrode resistance for a two-layer case with respect to layer thickness and conductivity ratio. We found that there is a saturation effect with respect to the conductivity of the first layer, i.e. when trying to improve contact resistance by watering the electrode, there is a maximum fluid conductivity beyond which the resistance cannot be further improved. We also found that the sensitivity range when trying to determine the halfspace resistivity from impedance measurements, is approx. 10 electrode radii.

For capacitively coupled electrodes, the common assumption of an ideal conductor breaks down for resistive ground and high frequencies. Depending on electrode size and geometry, the electrode impedance may be underestimated by two orders of magnitude if the finite conductivity is neglected.

The transition between the impedance of a capacitively coupled disc and a galvanically coupled disc lying on the ground is continuous as function of distance. Depending on the subsurface parameters, however, the transition may take place at extremely small distances in the order of an atomic radius, and thus will appear as a discontinuity in practice. The magnitude is monotonically increasing with distance, which means that the impedance of a capacitively coupled electrode can never be smaller than that of the same electrode lying on the ground. In practice, it may still be useful to insulate an electrode. For example, for a moving system, the large impedance variations with distance may cause problems for the electronics, in which case an insulation will stabilize the impedance.

The measurement of ground parameters is normally carried out with four-electrode arrays, not only on earth, but also on planetary probes (e.g. Hamelin *et al.* 2004; Seidensticker *et al.* 2007). The four-electrode transfer impedance does not depend on the contact impedance of the electrodes, provided that the contact impedances are small compared to the input impedance of the electronics. Here, we provide some simple tools to estimate contact impedances for a wide range of conditions, which may help to design electrodes such that difficulties with the electronics might be avoided. In addition, the contact impedance itself might be used to estimate ground parameters, either as a standalone system for shallow investigation in the range of electrode size, or as supplementary information for four-electrode arrays. The extra effort to measure contact impedances of an existing four-electrode array should be marginal compared to the initial expenses, in particular for planetary probes. In most cases, only a single four-electrode array will be used, and therefore the depth resolution obtained by using contact impedances might be extremely useful.

The estimation of ground parameters from the impedance may be disturbed by the dependence of the impedance on electrode height. We derived a simple rule for the maximum distance below which this dependence vanishes and where ground parameters can be determined without knowledge of electrode distance above ground. In the experiment we carried out to verify our numerical code, we probably did not reach this range due to the large values of frequency-dependent electrical permittivity, which dominates the corresponding equation.

The measured impedance is also influenced by internal capacitances of the measurements system. In our experiments we calibrated the configuration in the air, whereas Dashevsky *et al.* (2005) suggested to measure the vertical gradient of the contact impedance. They also used 3-D numerical modelling to calculate the impedance of the entire system. Such complex simulations might in future be supported or verified by our analytical and semi-analytical solutions.

ACKNOWLEDGMENTS

We thank Oliver Kuras, the editor, Oliver Ritter, and an anonymous reviewer for useful comments and suggestions on an earlier version of the manuscript.

The work was partly sponsored by the German research Foundation (project Ho1506/22–1).

REFERENCES

Chelidze, T.L., Gueguen, Y. & Ruffet, C., 1999. Electrical spectroscopy of porous rocks: a review – II. Experimental results and interpretation, *Geophys. J. Int.,* **137,** 16–34.

Dashevsky, Y.A., Dashevsky, O.Y., Filkovsky, M.I. & Synakh, V.S., 2005. Capacitance sounding: a new geophysical method for asphalt pavement quality evaluation, *J. Appl. Geophys.,* **57,** 95–106.

Grard, R. & Tabbagh, A., 1991. A mobile four-electrode array and its application to the electrical survey of planetary grounds at shallow depths, *J. geophys. Res.,* **96,** 4117–4123.

Hamelin, M., Grard, R., Laakso, H., Ney, R., Schmidt, W. & Trautner, R., 2004. Conductivity and dielectric characteristics of planetary surfaces measured with mutual impedance probes. From HUYGENS and Rosetta Lander to netlanders and future missions, *European Space Agency, Special Publication,* **543,** 16–172.

Krajew, A.P., 1957. *Grundlagen der Geoelektrik,* VBM Verlag Technik, Berlin.

Kuras, O., Beamish, D., Meldrum, P.I. & Ogilvy, R.D., 2006. Fundamentals of the capacitive resistivity technique, *Geophysics,* **71,** G135–G152.

Kuras, O., Meldrum, P.I., Beamish, D., Ogilvy, R.D. & Lala, D., 2007. Capacitive resistivity imaging with towed arrays, *J. Environ. Eng. Geophys.,* **12,** 267–279.

Lesmes, D.P. & Morgan, F.D., 2001. Dielectric spectroscopy of sedimentary rocks, *J. geophys. Res.,* **106,** 13329–13346.

Maley, S.W. & King, R.J., 1961. Impedance of a monopole antenna with a circular conducting-disc ground system on the surface of a lossy half space, *J. Res. Nat. Bur. Stand, Sec. D. Radio Prop.,* **65D,** 183–188.

Rücker, C. & Günther, T., 2011. The simulation of finite ERT electrodes using the complete electrode model, *Geophysics,* **76,** F227–F238.

Seidensticker, K.J. *et al.*, 2007. SESAME – an experiment of the ROSETTA Lander Philae: objectives and general design, *Space Sci. Rev.,* **128,** 301–337.

Smythe, W.R., 1968. *Static and Dynamic Electricity,* 3rd edn, McGRaw-Hill, New York.

Spitzer, K., Sohl, F. & Panzner, M., 2008. Numerical simulation of a permittivity probe for measuring the electrical properties of planetary regolith and application to the near-surface region of asteroids and comets, *Met. Planet. Sc.,* **43**(6), 997–1007.

Stillman, D.E., Grimm, R.E. & Dec, S.E., 2010. Low-frequency electrical properties of ice-silicate mixtures, *J. Phys. Chem. B,* **114,** 6065–6073.

Wait, J.R. & Pope, W.A., 1954. The characteristics of a vertical antenna with a radial conductor ground system, *Appl. Sci. Res.,* **B4,** 177–195.

APPENDIX: IMPEDANCE OF A CIRCULAR DISC OVER A HOMOGENEOUS HALFSPACE

A1 Basic equations

In order to calculate the electric field on the circular disc, we solve Maxwell's equations in cylindrical coordinates. Ampere's law for harmonic time dependence yields:

$$\sigma \mathbf{E} + \frac{\partial \varepsilon \mathbf{E}}{\partial t} = (\sigma + i\omega\varepsilon)\,\mathbf{E} = \bar{\sigma}\mathbf{E} = \nabla \times \mathbf{H} \tag{A1}$$

with electric and magnetic fields ***E*** and ***H***. The electrical conductivity and permittivity depend only on the vertical coordinate z. For symmetry reasons, the electric field only has a vertical and a radial component, which depend only on r and z. The magnetic field only has a tangential component H_φ that only depends on r and z. Therefore, from eq. (A1) we obtain for the remaining components:

$$\bar{\sigma}\, E_r = -\frac{\partial H_\varphi}{\partial z}, \tag{A2}$$

$$\bar{\sigma}\, E_z = \frac{1}{r}\frac{\partial \left(r H_\varphi\right)}{\partial r}. \tag{A3}$$

Similarly, from the law of induction:

$$-\frac{\partial \mathbf{B}}{\partial t} = \nabla \times \mathbf{E}, \tag{A4}$$

we obtain:

$$-i\omega\mu_0 H_\varphi = -\frac{\partial E_z}{\partial r} + \frac{\partial E_r}{\partial z}, \tag{A5}$$

where μ_0 is free-space magnetic permittivity. Substitution of (A2) and (A3) into (A5) yields an equation for H_φ:

$$\partial_r\left(\frac{1}{r}\partial_r\left(r H_\varphi\right)\right) + \bar{\sigma}\,\partial_z\left(\frac{1}{\bar{\sigma}}\partial_z H_\varphi\right) = i\omega\mu_0\bar{\sigma}\, H_\varphi. \tag{A6}$$

Here and subsequently we use the notation $\partial_r = \frac{\partial}{\partial r}$ for simplicity.

The left hand side of eq. (A6) suggests a separation of variables by means of a first order Bessel function, with wavenumber u:

$$H_\varphi(r, z) = f(z, u) \cdot J_1(ur). \tag{A7}$$

Because the Bessel function fulfils Bessel's differential equation

$$\frac{\partial_r J_1(ur)}{r} + \partial_r^2 J_1(ur) - \frac{1}{r^2} J_1(ur) = -u^2 J_1(ur) \tag{A8}$$

it follows from (A7) that

$$\partial_r\left(\frac{1}{r}\partial_r\left(r H_\varphi\right)\right) = -u^2 H_\varphi. \tag{A9}$$

The full solution of (A6) may thus be represented by an integration over all wavenumbers:

$$H_\varphi(r, z) = \int_0^\infty f(z, u) J_1(ur)\, du. \tag{A10}$$

From Ampere's law (A2 and A3) we directly obtain equations for the components of the electric field:

$$E_r(r, z) = \frac{-1}{\bar{\sigma}} \int_0^\infty \frac{\partial f(z, u)}{\partial z} J_1(ur)\, du, \tag{A11}$$

$$E_z(r, z) = \frac{1}{\bar{\sigma}} \int_0^\infty u f(z, u) J_0(ur)\, du. \tag{A12}$$

A2 Calculation of *f(z,u)*

If we substitute eq. (A10) in eq. (A6) it follows from eq. (A9) that *f(z,u)* must fulfil:

$$\bar{\sigma}\,\partial_z\left(\frac{1}{\bar{\sigma}}\partial_z f\right) = \alpha^2 f, \tag{A13}$$

where

$$\alpha^2 = i\omega\mu_0\bar{\sigma} + u^2. \tag{A14}$$

The electric field eq. (A12) has to be solved under the boundary conditions at layer boundaries and the source condition, which is

implemented by a jump in the vertical component of the electric field at the disc:

$$[E_z(r)]_-^+ = \frac{q(r)}{\varepsilon_0}, \tag{A15}$$

where $[]_-^+$ denotes the difference of the field immediately above and below the disc, i.e. the jump in the field:

$$[E]_-^+ = E\left(z = 0^+\right) - E\left(z = 0^-\right). \tag{A16}$$

To derive a condition for *f(r,z),* we transform eq. (A15) into the wavenumber domain by eq. (A12) and obtain:

$$[E_z(r,z)]_-^+ = \frac{1}{\bar{\sigma}_0}\int_0^\infty u\,[f(z,u)]_-^+ J_0(ur)\,du = \begin{cases} \frac{q(r)}{\varepsilon_0}, 0 \le r \le a \\ 0, r > a \end{cases}, \tag{A17}$$

where σ_0 is the free-space conductivity. The charge density $q(r)$ may be transformed to the wavenumber domain through the Hankel transform pair:

$$\tilde{q}(u) = \int_0^\infty uq(r)\,J_0(ur)\,dr, \tag{A18}$$

$$q(r) = \int_0^\infty u\tilde{q}(u)\,J_0(ur)\,du, \tag{A19}$$

where $\tilde{q}(u)$ is the charge density in the wavenumber domain.

By substituting eq. (A19) into (A17) it becomes obvious that

$$[f(z,u)]_-^+ = \frac{\bar{\sigma}_0}{\varepsilon_0}\tilde{q}(u) \tag{A20}$$

is the boundary condition describing the source in the wavenumber domain.

Eq. (A13) has to be solved under the boundary condition (A20). Solutions will be linear combinations of functions of the form $e^{\pm\alpha z}$, where the different values of α in the lower halfspace and in the air have to be considered. This suggests the following Ansatz for *f(z,u)*:

$$f(z,u) = \begin{cases} -Ae^{+\alpha_0 z} + Be^{+\alpha_0 z}, z < 0 \\ +Ae^{-\alpha_0 z} + Be^{+\alpha_0 z}, 0 < z < d \\ Ce^{-\alpha_1 z}, z > d \end{cases}, \tag{A21a,b,c}$$

where

$$\alpha_0^2 = i\omega\mu_0\bar{\sigma}_0 + u^2 \; and \; \alpha_1^2 = i\omega\mu_0\bar{\sigma}_1 + u^2 \tag{A22a,b}$$

are the corresponding parameters in the air and in the halfspace. The signs of the exponents in eq. (21) result from the request that *f(z,u)* has to vanish at infinity in both directions. The constants *A, B* and *C* can be determined from the source condition (A20) and the continuity conditions for the electromagnetic fields at layer boundaries, which mean that *f* and $\frac{1}{\bar{\sigma}}\frac{\partial f}{\partial z}$ have to be continuous. For example, it follows from (A21a,b), that

$$\begin{aligned} f\left(z = 0^-\right) &= B - A \\ f\left(z = 0^+\right) &= A + B \end{aligned}. \tag{A23a,b}$$

And thus for the jump of *f* at $z = 0$*:*

$$[f(z,u)]_-^+ = f\left(z = 0^+\right) - f\left(z = 0^-\right) = 2A. \tag{A24}$$

With eq. (A20), we obtain for constant A:

$$A = \frac{\bar{\sigma}_0}{2\varepsilon_0}\tilde{q}(u). \tag{A25}$$

The calculation of B and C is also straightforward but requires a little more algebra that is omitted here. The final result for *f* is:

$$f(z,u) = \frac{\bar{\sigma}_0}{2\varepsilon_0}\tilde{q}(u)\begin{cases} e^{+\alpha_0 z} + R(u)\,e^{\alpha_0(z-2d)}, z < 0 \\ e^{-\alpha_0 z} + R(u)\,e^{\alpha_0(z-2d)}, 0 < z < d \\ T(u)\,e^{-\alpha_1(z-d)}e^{-\alpha_0 d}, z > d \end{cases} \tag{A26a,b,c}$$

with reflection and transmission factors:

$$R(u) = \frac{\alpha_0(u)\,\bar{\sigma}_1 - \alpha_1(u)\,\bar{\sigma}_0}{\alpha_0(u)\,\bar{\sigma}_1 + \alpha_1(u)\,\bar{\sigma}_0}, \tag{A27}$$

$$T(u) = \frac{2\alpha_0(u)\,\bar{\sigma}_1}{\alpha_0(u)\,\bar{\sigma}_1 + \alpha_1(u)\,\bar{\sigma}_0}. \tag{A28}$$

With eq. (A26)–(A28) and (A10)–(A12) we could in principle calculate all field components. However, in order to calculate the charge density on the disc, we need only the equation for E_r between the halfspace and the disc. In the following, we approximate α between the halfspace and the disc by the wavenumber u, i.e.:

$$\alpha_0^2 = u^2 + \omega^2\mu_0\varepsilon_0 = u^2 + \frac{\omega^2}{c^2} \approx u^2, \tag{A29}$$

where c is the vacuum speed of light. The approximation is justified, because the minimum relevant wavenumber $u_{\min}$ is given by the inverse size of the disc, which is large compared to the electromagnetic (EM) wavenumber in free space (i.e. the second term on the R.H.S. of eq. (A29). For example, even for a large electrode with 1m radius operating at a maximum frequency of 10 MHz, the ratio between EM wavenumber and $u_{\min}$ is only 0.04.The equation for E_r is obtained from (A26b) and (A12), considering that the derivative with respect to z gives a multiplication with u:

$$E_r(r,z) = \frac{1}{2\varepsilon_0}\int_0^\infty u\tilde{q}(u)\left[e^{-uz} - R(u)\,e^{u(z-2d)}\right] \times J_1(ur)\,du,\ 0 \le z \le d. \tag{A30}$$

A3 Calculation of the charge density

To calculate the charge density, we utilize the condition that the radial electric field has to vanish on the disc. Thus, we need the field at $z = 0$:

$$E_r(r, z = 0) = \frac{1}{2\varepsilon_0}\int_0^\infty u\tilde{q}(u)\left[1 - R(u)\,e^{-2ud}\right]J_1(ur)\,du. \tag{A31}$$

The idea is to find a charge distribution that fulfils $E_r = 0$ for any *r.* If we substitute the tranformation of the charge density (eq. 18) into eq. (A31), we obtain:

$$\frac{1}{2\varepsilon_0}\int_0^\infty\int_0^a sq(s)\,J_0(s)u\left[1 - R(u)\,e^{-2ud}\right]J_1(ur)\,du\,ds = 0 \tag{A32}$$

with the new integration variable s. One may write eq. (A32) more compactly by defining the function

$$F(s,r) = \int_0^\infty u\left[1 - R(u)\,e^{-2ud}\right]J_0(us)\,J_1(ur)\,du \tag{A33}$$

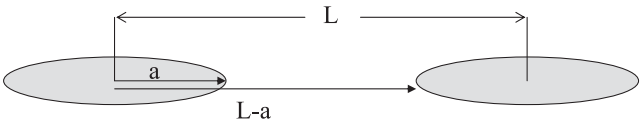

Figure A1. Geometry of the transmitting system consisting of two identical discs. The distance between the midpoints is L, the radius of the discs is a.

to obtain

$$\frac{1}{2\varepsilon_0}\int_0^a sq\,(s)\,F\,(s,r)\,ds = 0. \tag{A34}$$

The function *F(s,r)* may be directly calculated for any s and r. For numerical implementation, the disc may be discretized and with discrete values we obtain a matrix **F.** Eq. (A34) then becomes a system of linear equations:

$$\mathbf{F}\cdot\mathbf{q} = \mathbf{0}, \tag{A35}$$

where the entries into vector **q** represent the unknown charge density distribution. However, **q** is not yet completely defined by eq. (A35), because it has a trivial solution $\mathbf{q} = \mathbf{0}$. The potential of the disc has to be included as a further constraint to obtain a finite charge. One possibility to include the potential is to consider a system consisting of two identical discs (Fig. A1).

Integration of E_r along the line connecting the midpoints of the two discs yields the applied voltage V_0. Since $E_\mathrm{r} = 0$ on the discs, this is:

$$V_0 = \int_a^{L-a} [E_r\,(r,0) + E_r\,(L-r,0)]\,dr = 2\int_a^{L-a} E_r\,(r,0)\,dr. \tag{A36}$$

E_r(r,0) is given by eq. (A31) and can be substituted directly. Carrying out the integration over r, we obtain:

$$\begin{aligned} V_0 &= 2\int_a^{L-a}\frac{1}{2\varepsilon_0}\int_0^\infty u\tilde{q}\,(u)\left[1 - R\,(u)\,e^{-2ud}\right]J_1\,(ur)\,du dr \\ &= \frac{1}{\varepsilon_0}\int_0^\infty u\tilde{q}\,(u)\left(1 - R\,(u)\,e^{-2ud}\right)\left[\int_a^{L-a} J_1\,(ur)dr\right]du \\ &= \frac{1}{\varepsilon_0}\int_0^\infty \tilde{q}\,(u)\left(1 - R\,(u)\,e^{-2ud}\right)[J_0\,(ua) - J_0\,(u\,(L-a))]\,du \end{aligned} \tag{A37}$$

In order to define an explicit discretization, the charge density is written in space domain, and the equation is written as:

$$\begin{aligned} V_0 &= \frac{1}{\varepsilon_0}\int_0^\infty\int_0^a sq\,(s)J_0\,(us)\,ds\left(1 - R\,(u)\,e^{-2ud}\right) \\ &\quad\times[J_0(ua) - J_0(u(L-a))]du \\ &= \frac{1}{\varepsilon_0}\int_0^a sq\,(s)\,G\,(s)ds \end{aligned}, \tag{A38}$$

where

$$G\,(s) = \int_0^\infty \left(1 - R\,(u)\,e^{-2ud}\right)J_0\,(us)\,[J_0\,(ua) - J_0\,(u\,(L-a))]\,du \tag{A39}$$

is a new function that can be calculated for any s. Again, eqs (A38) and (A39) are discretized and converted into a linear equation system of the form:

$$\mathbf{q}\cdot\mathbf{G} = V_0. \tag{A40}$$

Eq. (A40) is the inhomogeneous condition that is required to exclude the trivial solution. Any value for V_0 may be chosen to obtain a charge density distribution *q(r)* by solving eq. (A35) under the condition (A40). The total charge is obtained from eq. (8) of the main section, and the capacitance from eq. (9). Although the distance between the discs L appears as a parameter in the equations, the solution does not depend on the choice and any value $L > 2a$ may be chosen for the numerical implementation.

For a system consisting of two discs, the solution is valid only at sufficient distance of the two discs, because the mutual influence was not considered here. The capacitance of the electrode C is complex, because the reflection factor in eq. (A27) is complex. The complex electrode impedance may be calculated via

$$Z = \frac{1}{i\omega C}. \tag{A41}$$